Advanced 3D Models of Potential Lava Tubes on the Moon from Inversion of GRAIL Gravity Data

Meixia Geng[1*], Qingjie Yang[1], Chaouki Kasmi[1], J. Kim Welford[2], Alexander L. Peace[3], Ruiyuan Kang[1]

1 Directed Energy Research Centre, Technology Innovation Institute, Abu Dhabi, UAE.

2 Memorial University of Newfoundland, Department of Earth Sciences, St. John's, Newfoundland and Labrador, Canada.

3 School of Earth, Environment and Society, McMaster University, Hamilton, ON L8S 4K1, Canada.

Email: meixia.geng@tii.ae

Abstract

Lunar lava tubes, formed by volcanic activity, present potential habitats for future human exploration due to their stable environments. This research uses a 3D inversion technique to detect these tubes by analyzing gravity anomalies from NASA's GRAIL mission. Four potential regions were modeled, with two main candidates located at Schröter extension and Rima Mairan. These models reveal extensive underground networks, with the Schröter extension tube spanning 63 km and the Rima Mairan tube extending 160 km. The study's 3D models, enhanced by LRO topographical data, provide critical insights for future lunar exploration and habitation planning.

Introduction

Lunar lava tubes are underground channels formed by volcanic activity during the Moon's volcanic period. These intact structures have the potential to serve as secure shelters for human habitation and facilities, providing a stable environment with a constant temperature. Due to their lower density compared to surrounding rocks, lunar lava tubes can be detected using their gravity anomalies. By applying a 3D inversion technique to gravitational gradient data derived from NASA's GRAIL (Gravity Recovery and Interior Laboratory) mission, we have constructed detailed 3D density models of potential lava tubes, enhancing our understanding of these intriguing geological features and their geometries.

Efforts[1, 2, 3, 4, 5, 6, 7, 8] have been made to identify cave conduits near pits using nadir-looking orbital ground-penetrating radar, gravimeters, and radiometers. However, the results of these experiments remain inconclusive. Direct exploration could confirm the presence of stable subsurface environments shielded from radiation and with optimal temperature conditions for future human utilization. Yet, such robotic missions would face significant challenges in navigating unknown terrains without available predictions regarding the extent and morphology of these conduits. Therefore, it is crucial to identify and establish a 3D model of the lava tubes for lunar exploration.

Methodology

The 3D inversion technique applied in this research is based on the probabilistic method[9] to generate 3D density models by inverting gravity/gravity gradient data. The method was assessed and proven successful in identifying the density structures of both the upper and lower crust of the Earth [10, 11, 12, 13, 14, 15, 16, 17]. A significant advantage of this inversion approach is its capacity to integrate a priori information regarding physical properties, spatial extent, depth, and orientation of the source body via the covariance matrix to construct an accurate and reliable solution.

The objective function employed for the inversion of gravity data is based on a probabilistic inversion method[9]:

$$\mathbf{\Phi} = (\mathbf{Gm} - \mathbf{d}_{\mathrm{obs}})^T \mathbf{C}_{\mathrm{D}}^{-1}(\mathbf{Gm} - \mathbf{d}_{\mathrm{obs}}) + (\mathbf{m} - \mathbf{m}_{\mathrm{apr}})^T \mathbf{C}_{\mathrm{M}}^{-1}(\mathbf{m} - \mathbf{m}_{\mathrm{apr}}). \qquad (1)$$

Here, $\mathbf{m}$ represents the model parameter vector, values of the densities of the cells, $\mathbf{d}$ is the gravity data vector, and $\mathbf{G}$ is the forward modeling matrix where $\mathbf{Gm} = \mathbf{d}$. The first term of equation (1) signifies the data misfit function, weighted by the data error covariance matrix, $\mathbf{C}_{\mathrm{D}}$. The second term corresponds to the stabilizing function, which accounts for the deviation of model parameters $\mathbf{m}$ from a reference model $\mathbf{m}_{\mathrm{apr}}$, weighted by the model covariance matrix $\mathbf{C}_{\mathrm{M}}$. To minimize the objective function, the solution is derived below[9]

$$\widetilde{\mathbf{m}} = \mathbf{m}_{\mathrm{apr}} + \mathbf{C}_{\mathrm{M}}\mathbf{G}^T(\mathbf{G}\mathbf{C}_{\mathrm{M}}\mathbf{G}^T + \mathbf{C}_{\mathrm{D}})^{-1}(\mathbf{d}_{\mathrm{obs}} - \mathbf{Gm}_{\mathrm{apr}}). \qquad (2)$$

To counteract the natural decay of the forward modeling matrix with increasing depth, a depth weight function with the following form was used:

$$w(z) = 1/(z_{\mathrm{max}} - z)^{\beta}, \qquad (3)$$

where z_{max} is the maximum depth of the inversion domain and z is the depth of each cell. β is the exponent of the depth weight function and typically ranges from 1 to 3. The solution with the depth-weighting function is:

$$\tilde{\mathbf{m}} = \mathbf{m}_{apr} + \mathbf{W}^{-1}\mathbf{C}_M\mathbf{W}^{-1}\mathbf{G}^T(\mathbf{G}\mathbf{W}^{-1}\mathbf{C}_M\mathbf{W}^{-1}\mathbf{G}^T + \mathbf{C}_D)^{-1}(\mathbf{d}_{obs} - \mathbf{G}\mathbf{m}_{apr}). \qquad (4)$$

Results

To identify and analyze potential lava tube locations, we developed four distinct density models for different regions that were identified as lava tube candidates. Our 3D inversion density models indicate a high likelihood of lava tubes in two primary areas: Schröter extension (W54°, N24°) and Rima Mairan (W46°, N36°). The candidate lava tube (Figure 1) in the Schröter extension spans 63 km in length and approximately 400 m in height, which suggests it could be an extension of the Schröter Rill, a prominent sinuous rille, or depression, on the lunar surface. The second area, Rima Mairan, lies near two known sinuous rilles, specifically south of Rima Sharp and west of Rima Mairan. The candidate lava tube (Figure 2) in this region extends 160 km in total length with a height of up to 300 m. This extensive structure is divided into western and eastern segments by a high-density anomaly. The western segment measures approximately 56 km and is oriented WNW-ESE, while the eastern segment measures about 94 km and is oriented W-E. These findings highlight a potentially vast underground network that could be utilized for future lunar exploration and habitation.

Our 3D models are consistent with previous length and height estimations obtained from forward modeling techniques, yet they provide a more detailed spatial distribution of the lava tubes. This enhanced detail is made possible by the integration of topographical data from the Lunar Reconnaissance Orbiter (LRO) mission, which allows for more accurate and comprehensive modeling. These sophisticated 3D models are essential for understanding the formation and distribution of lunar lava tubes and play a vital role in planning future lunar stations.
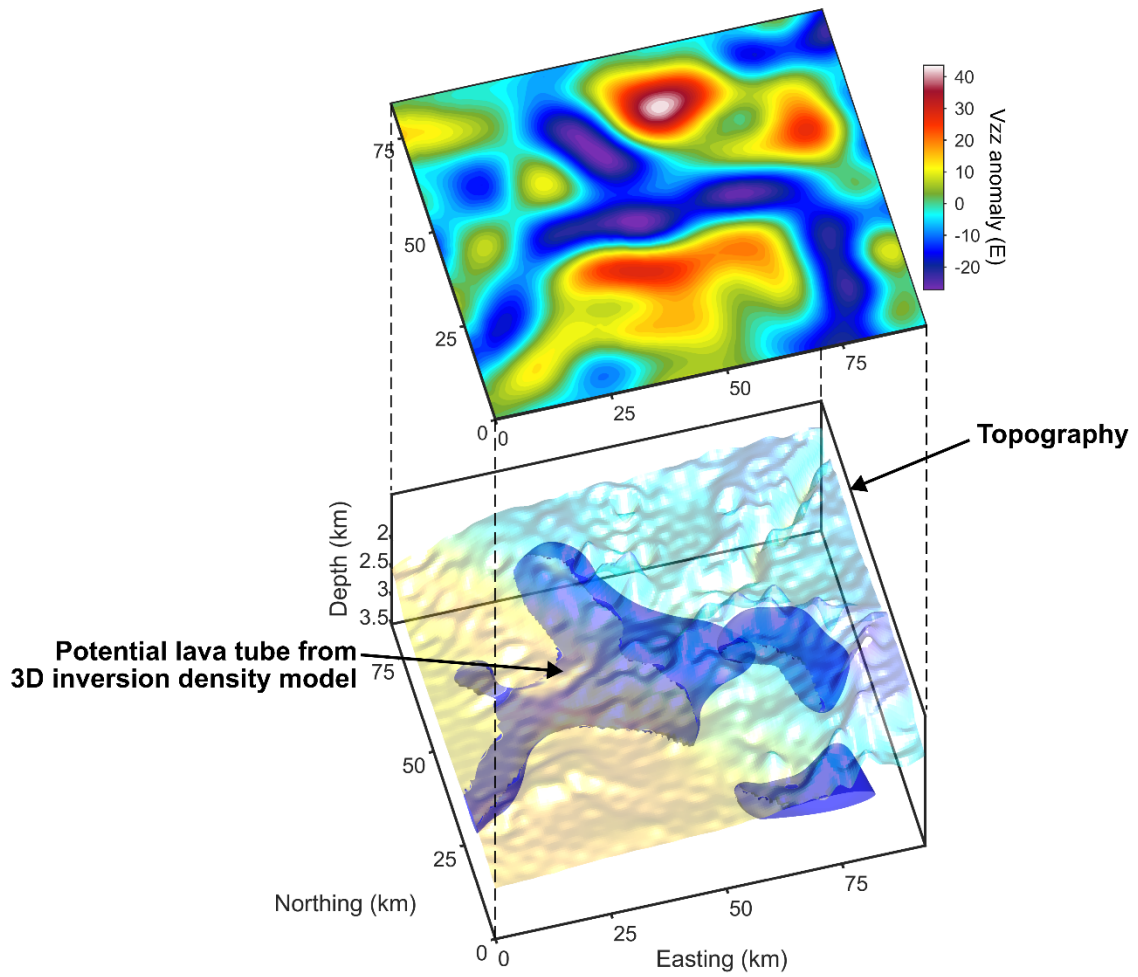
Figure 1. Gravity gradient anomaly in Schröter extension region derived from NASA's GRAIL mission and 3D density model from inversion, which is shown in the blue bodies and interpreted as potential lava tube.

Figure 2. Gravity gradient anomaly in Rima Mairan region derived from NASA's GRAIL mission and 3D density model from inversion, which is shown in the blue bodies and interpreted as potential lava tube.
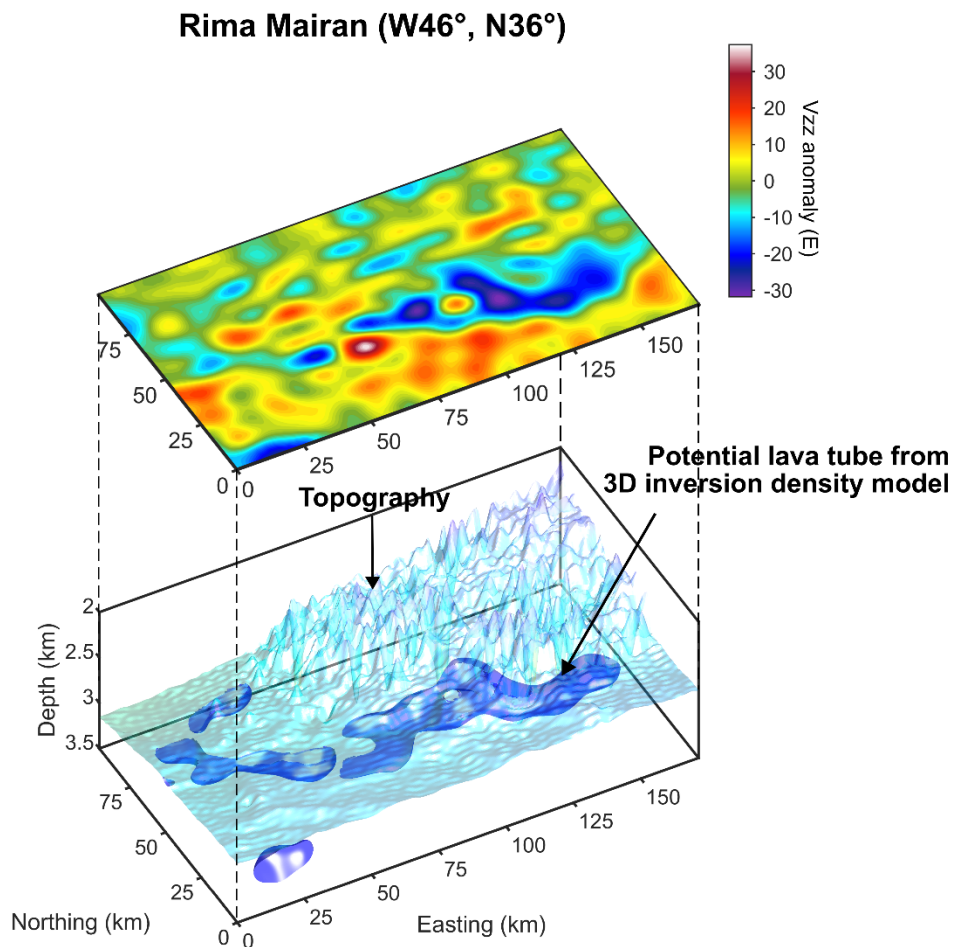
References

1. Carrer L, Pozzobon R, Sauro F, Castelletti D, Patterson GW, Bruzzone L. Radar evidence of an accessible cave conduit on the Moon below the Mare Tranquillitatis pit. *Nature Astronomy*, 1-8 (2024).

2. Chappaz L, *et al.* Evidence of large empty lava tubes on the Moon using GRAIL gravity. *Geophysical Research Letters* **44**, 105-112 (2017).

3. Donini E, Carrer L, Gerekos C, Bruzzone L, Bovolo F. An unsupervised fuzzy system for the automatic detection of candidate lava tubes in radar sounder data. *IEEE Transactions on Geoscience and Remote Sensing* **60**, 1-19 (2021).

4. Haruyama J*, et al.* Possible lunar lava tube skylight observed by SELENE cameras. *Geophysical Research Letters* **36**, (2009).

5. Horvath T, Hayne PO, Paige DA. Thermal and illumination environments of lunar pits and caves: Models and observations from the Diviner Lunar Radiometer experiment. *Geophysical Research Letters* **49**, e2022GL099710 (2022).

6. Kaku T*, et al.* Detection of intact lava tubes at Marius Hills on the Moon by SELENE (Kaguya) Lunar Radar Sounder. *Geophysical Research Letters* **44**, 10,155-110,161 (2017).

7. Wilcoski A, Hayne P, Elder C. Thermal environments and volatile stability within lunar pits and caves. *Journal of Geophysical Research: Planets* **128**, e2023JE007758 (2023).

8. Zhu K, Yang M, Yan X, Li W, Feng W, Zhong M. GRAIL gravity gradients evidence for a potential lava tube at Marius Hills on the moon. *Icarus* **408**, 115814 (2024).

9. Tarantola A. *Inverse problem theory and methods for model parameter estimation*. siam (2005).

10. Ali MY, Geng M, Fairhead JD, Adan A. 3D constrained inversion of gravity and magnetic data to image basement and plutonic bodies: A case study from Dood Arale Basin, eastern Somaliland. *Geophysics* **86**, B321-B334 (2021).

11. Geng M, Ali MY, Fairhead JD, Pilia S, Bouzidi Y, Barkat B. Crustal structure of the United Arab Emirates and northern Oman Mountains from constrained 3D inversion of gravity and magnetic data: The Moho and basement surfaces. *Journal of Asian Earth Sciences* **231**, 105223 (2022).

12. Geng M, Ali MY, Fairhead JD, Pilia S, Bouzidi Y, Barkat B. Hormuz salt distribution in the United Arab Emirates: Implications for the location of hydrocarbon fields. *Marine and Petroleum Geology* **143**, 105797 (2022).

13. Peace AL, Welford JK, Geng M, Sandeman H, Gaetz BD, Ryan SS. Rift-related magmatism on magma-poor margins: Structural and potential-field analyses of the Mesozoic Notre Dame Bay intrusions, Newfoundland, Canada and their link to North Atlantic Opening. *Tectonophysics* **745**, 24-45 (2018).

14.   Welford JK, Peace AL, Geng M, Dehler SA, Dickie K. Crustal structure of Baffin Bay from constrained three-dimensional gravity inversion and deformable plate tectonic models. *Geophysical Journal International* **214**, 1281-1300 (2018).

15.   Geng M, Ali MY, Fairhead JD, Bouzidi Y, Barkat B. Morphology of the basement and Hormuz salt distribution in offshore Abu Dhabi from constrained 3-D inversion of gravity and magnetic data. *Tectonophysics* **791**, 228563 (2020).

16.   Rimando J, Peace AL, Geng M, Verbaas J, Slade H. Structural Setting of the Sixtymile Gold District, Yukon, Canada: Insights into Regional Deformation and Mineralization from Field Mapping and 3D Magnetic Inversion. *Minerals* **12**, 291 (2022).

17.   Geng M, Welford JK, Farquharson CG, Peace AL. 3D inversion of airborne gravity gradiometry data for the Budgell Harbour Stock, Newfoundland: A case history using a probabilistic approach. *Geophysics* **84**, B269-B284 (2019).